Turk J Pharm Sci 2025;22(2):119-130
DOI: 10.4274/tjps.galenos.2025.02772

ORIGINAL ARTICLE

Effect of *Aegle marmelos* Extract-Phospholipid Complexes in Dextran Sulfate Sodium-Induced Ulcerative Colitis in Rats

Pooja Ganpat SWAMI, Dilesh Jagdish SINGHAVI*, Rajendra Onkarappa GANJIWALE

Institute of Pharmaceutical Education and Research, Wardha, India

ABSTRACT

Objectives: Ayurvedic texts mention the use of *Aegle marmelos* fruit in colitis and other gastrointestinal ailments. The polyphenolic contents of the fruit, however, have poor bioavailability, limiting their therapeutic use. The study aimed to develop and optimise the *A. marmelos* fruit extract-phospholipid (AMEP) complex to improve the oral bioavailability of the *A. marmelos* extract (AME), and compare the *in vivo* effect of AME and AMEP in dextran sulfate sodium (DSS)-induced ulcerative colitis in rats.

Materials and Methods: The research work is the first of its kind to use a hydroalcoholic extract of A. marmelos fruit in the preparation of phospholipid complexes for ameliorating UC. The complexes were prepared using the solvent evaporation method and optimised by Box-Behnken design. The work compares the *in vivo* activity of plain AME, its phospholipid complexes, and the standard drug (mesalamine) in the alleviation of chemical-induced colitis in rats. AMEP was optimised using response surface methodology by Box-Behnken design. AMEP was characterised using scanning electron microscopy, Fourier transform infrared spectroscopy, differential scanning calorimetry, zeta analysis, and particle size analysis. A DSS-induced rat model was used *in vivo* studies to mimic ulcerative colitis. The pathogenesis of the disease was assessed by evaluating the levels of oxidative stress markers [nitric oxide (NO), malondialdehyde (MDA), and superoxide dismutase (SOD) activity], cytokines [tumor necrosis factor-alpha (TNF-α) and interleukin-6 (IL-6)], disease activity index, colon length, and histopathology.

Results: The characterization confirmed the formation of AMEP, having a particle size of 673.6±4.30 nm, polydispersity index of 0.224±0.010, and zeta potential of -42.6 mV±0.51. The NO, MDA, TNF-α, and IL-6 levels were significantly reduced ($p<0.0001$, $p<0.005$, $p<0.0001$, $p<0.01$), and the SOD level was significantly increased ($p<0.05$) in AMEP-treated groups compared to the AME-treated groups.

Conclusion: These findings suggessts that AMEP has a powerful potential to reduce the levels of oxidative markers and inflammatory cytokines, making it a promising treatment for ulcerative colitis.

Keywords: *Aegle marmelos* extract, phospholipid-complex, ulcerative colitis, Box-Behnken design

INTRODUCTION

Ulcerative colitis (UC) is a chronic idiopathic inflammatory disease of the colon. It is marked by relapses and remissions of mucosal inflammation, commencing in the rectum and extending to the proximal sections of the colon.[1] UC causes long-lasting inflammation and ulcers in the large intestine and rectum. It affects the colon's innermost lining, and the symptoms develop over time. It commonly affects adults in the age group between 30 and 40 and can be debilitating, potentially leading to serious, life-threatening complications.[2]

The current treatment regimen for UC focuses entirely on inducing remission and preventing relapses.[3] The pathogenic

***Correspondence:** dileshsinghavi@rediffmail.com, **ORCID-ID:** orcid.org/0000-0002-2544-7226
Received: 29.11.2023, **Accepted:** 23.03.2025 **Publication Date:** 14.05.2025

Cite this article as: SWAMI PG, SINGHAVI DJ, GANJIWALE RO. Effect of Aegle marmelos extract-phospholipid complexes in dextran sulfate sodium-induced ulcerative colitis in rats. Turk J Pharm Sci. 2025;22(2):119-130

heterogeneity of UC makes single-target therapy a challenge, as evidenced by the recent failures of pharmacological therapies, including tumor necrosis factor-alpha (TNF-α), anti-integrin, and Janus kinase inhibitors.[4,5] Thus, it is necessary to find alternative treatment solutions with multiple therapeutic targets.[6] The ineffectiveness of treatments, especially in chronic cases, has led to increased use of complementary and alternative medicine, in which herbal products are commonly used, in UC.[7,8]

Few plant actives and extracts have shown activity against UC, but often their usage is limited due to a lack of supporting studies.[9] *Aegle marmelos* (L.) Correa (Rutaceae) is one such plant used in the treatment of colitis and other gastroenterological disorders.[10] *A. marmelos* fruit has medicinal importance as an astringent, digestive, and stomachic agent.[11] Qualitative analysis of *A. marmelos* fruit extract (AME) confirms the presence of phenols, tannins, coumarin glycosides, flavonoids, and alkaloids. Gallic acid, quercetin, chlorogenic acid, ellagic acid, ferulic acid, kaempferol, and protocatechuic acid are some of the phenols and flavonoids reported to have been found in *A. marmelos* fruit. These compounds are profoundly important due to their antioxidant properties. However, the bioavailability of most of these compounds is poor, which limits their activity.[12,13]

A. marmelos fruit also shows the presence of marmelosin, which is a furanocoumarin (also a marker compound) with immunomodulatory potential that has antioxidant, antiproliferative, and anti-inflammatory activity.[14] It has been demonstrated that marmelosin alleviates inflammation by inhibiting the phosphorylated phosphoinositide 3-kinases/protein kinase B/nuclear factor-kappa B (PI3K/Akt/NF-κB) pathway.[15,16] It has been shown to alleviate UC symptoms by regulating the nuclear factor erythroid-2-related factor 2/antioxidant response elements/heme oxygenase-1 (Nrf-2/ARE/HO-1) pathway.[17] However, the bioavailability of marmelosin is poor, and it belongs to the Biopharmaceutics Classification System Class II category.[18]

The problem of poor bioavailability and solubility can be overcome using a method of lipid-based formulation developed recently, in which plant extracts or actives are complexed with dietary phospholipids.[19,20] The lipid-based formulations improve the solubility, oral absorption, and permeation of the actives without compromising their safety.[21,22] In the current study, we focused on preparing a cost-effective product for alleviating UC. The AME was prepared using aqueous ethanol. Since the extract contains various polyphenols, antioxidant and anti-inflammatory activity *via* multiple pathways can be achieved against colitis. The aim of the study was to formulate AMEP to enhance the solubility and absorption of the phytoactives of AME and to compare the effects of AME and AMEP (at the same dose) on rats with UC.

MATERIALS AND METHODS

Materials and reagents

Fresh fruits of *A. marmelos* were collected in January from Borgaon village in the Wardha district of Maharashtra, which had well-drained black soil. The specimens were authenticated [herb. Sheet no. Bot. Sp. 04/2020-21]. The specimen was authenticated by Dr. L.P Dalal, Head of the Department of Botany in Bajaj College of Science, Wardha, and deposited in Bajaj College of Science, Wardha. The fruits were cleaned, chopped, dried, and ground using a grinder. The resulting powder was sifted through a size #22 mesh and stored under cool and dry conditions.

A reference standard of marmelosin was obtained from Natural Remedies (Bangalore, India). Mesalamine tablets were obtained from Sun Pharmaceutical Industries Ltd. (India). 2,2-diphenyl-1-picrylhydrazyl and quercetin were bought from Research-Lab (Mumbai) and Chemika-Biochemika Reagents, respectively. Dextran sulfate sodium (DSS) was procured from Sisco Research Laboratories. Lipoid H90 was obtained as a sample from Lipoid GmbH, Ludwigshafen. Loba Chemie Pvt. Ltd. supplied the remaining chemicals.

Preparation of AME

AME was extracted using the maceration method from the powdered *A. marmelos* fruits. It was obtained using aqueous ethanol (50% *v/v*) with a 1:10 ratio of solute to solvent. It was filtered, dried, and stored in a desiccator.

Determination of marmelosin content in AME

The marmelosin content of the AME was determined through high-performance thin-layer chromatography (HPTLC) analysis. The samples were applied to pre-coated silica plates (F254, Merck) using Linomat5 (software WINCATS); a scanner (CAMAG-3) was utilised for scanning. *n*-Hexane and ethyl acetate 12:4 were used to make the mobile phase. A standard calibration curve was plotted using marmelosin solutions of concentrations 100, 200, 300, 400, and 500 µg/mL.

AME sample solutions with a concentration of 100 mg/mL were prepared. Each sample of 10 µL was applied on the silica plate, which was run in a twin-trough chamber. The plate was developed using 10% *w/v* methanolic potassium hydroxide (KOH). Peaks were recorded at 366 nm using a TLC scanner. Quantification was done using the calibration curve of marmelosin ($y=11.63x+431.5$; $R^2=0.999$), which was expressed as mg/g of extract.

Preparation and optimization of AMEP

AMEP was prepared using the solvent evaporation method and a rotary evaporator.[23] In brief, AME and PC were dispersed in absolute ethanol in a round-bottom flask in different ratios and stirred for 1-3 hours at a temperature between 35 °C and 45 °C. The solvent was then evaporated using an evaporator. The complexes were then removed and allowed to dry. The samples were then stored in desiccators.

A QbD-based approach using a Box-Behnken formulation design was used to obtain a response surface for optimization of phospholipid complexes. The influences of three independent variables, namely, (1) AME-to-phospholipid ratio *(w/w)*, (2) reaction temperature (°C), and (3) reaction time (hours), on the dependent variable of the complex, *i.e.*, the entrapment efficiency (%), were studied. The experiments were designed

using the Design Expert software package (Version 13.0.5.0, StatEase Inc.). Fifteen formulations were designed, with one centre point.

Entrapment efficiency (EE) of AMEP

The EE of the marker compound, marmelosin, was determined in the AMEP using the HPTLC method. AME and AMEP samples were prepared at a concentration of 10 mg/mL. The samples (10 µL) were applied on pre-coated silica plates (F254, Merck), using Linomat5, and a CAMAG TLC scanner3 was used for scanning. The mobile phase consisted of a 1:1 mixture of n-hexane and ethyl acetate. The plate was run in a twin-trough glass chamber. Methanolic KOH (10% *w/v*) was used for sample derivatization, and peaks were recorded at 366 nm.

$$EE\ (\%) = \frac{Marmelosin\ content\ in\ AMEP}{Marmelosin\ content\ in\ AME} \times 100 \quad (1)$$

Characterization of optimised AMEP formulation

Solubility of AMEP

The solubility of the AMEP was checked in ethanol (50% *v/v*), absolute ethanol, ethyl acetate, chloroform, dimethyl sulfoxide, methanol, and water.

Particle size, polydispersity index (PI), and zeta potential

The particle size, PI, and zeta potential of the AMEP were determined by dynamic light scattering (DLS; Horiba-DLS-7100E, Japan). The AMEP was dispersed in water prior to analysis.

Fourier transform infrared spectroscopy (FTIR)

FTIR analysis was carried out using an infrared spectrophotometer (IR affinity, model 206-73500-38, Shimadzu). The potential interactions were investigated by comparing the IR spectra of PC, AME, physical mixture of PC and AME, and AMEP in the 4000-400 cm-1 wavenumber region.

Scanning electron microscopy (SEM)

The morphology of the AMEP was studied using a Hitachi High-Tech S3700N scanning electron microscope.

Differential scanning calorimetry (DSC)

Thermograms of PC, AME, PM, and AMEP were recorded using a differential scanning calorimeter (DSC-60, Shimadzu). A heating rate of 10 °C/minute was used for the thermal analysis. The percentage weight loss of the samples was monitored from 25 °C to 400 °C.

Experimental animals

In vivo investigations utilized male Wistar rats weighing 200-280 g. The animals were kept at standard temperature (25 °C) and light (12:12 hours of light-dark cycles) conditions. They were given access to water and food *ad libitum*. Practical procedures were performed in compliance with the CPCSEA, Government of India, and, as approved by the Institutional Animal Ethic Committee study protocol (approval number: 535/PO/RERCBT/S/02/CPCSEA/IPER/IAEC/2020-2021/17, date: 19.12.2020).

Disease induction

A chemically induced colitis model was used. The animals were put into six groups at random, with six animals in each group: (1) the normal group (G-I), (2) the DSS group, or positive-control group (G-II), (3) the standard-treated group (mesalamine) [100 mg/kg body-weight (bw)] (G-III), (4) the AME-treated group (400 mg/kg bw) (G-IV), (5) the AMEP-treated group (800 mg/kg bw) (G-V), and (6) the excipient (PC) group (400 mg/kg bw) (G-VI).

Acute colitis was induced by the oral administration of 6% DSS (MW 50 kDa) in drinking water.[24] The animals of all groups except G-I were given 6% DSS in water *ad libitum* for 7 days. The animals developed severe diarrhoea and had significant weight loss. The animals of all groups (except G-I and G-II), were treated for the next 7 days with their respective treatments. Their weights were monitored, and their faeces were observed throughout the experiment.

The animals of each group were then sacrificed using the cervical dislocation method after being fasted overnight.[24] The colon was excised and cleaned with an ice-cold saline solution of 0.9% *w/v*. The colon tissues were stored in chilled phosphate-buffered saline (pH 7.4) for biochemical analysis.

Colon length and Disease Activity Index (DAI)

The length of the colon between the ileocecal junction and the proximal rectum was measured. Body weight, stool consistency, and gross rectal bleeding were noted. The DAI was used to evaluate the severity of the colitis.[25]

Biochemical evaluation

The rat colons were homogenized in ice-cold 0.01 M phosphate buffer (pH 7.4) at 4000 rpm for 15 minutes to obtain a 10% *w/v* homogenate. This was used to evaluate the antioxidant and anti-inflammatory activities in the colonic tissues. The colorimetric method was used for the analysis of nitric oxide (NO) content by the Montgomery method.[26] The superoxide dismutase (SOD) activity was determined using the Marklund and Marklund method,[27] and the malondialdehyde (MDA) activity was determined using the method of Okhawa et al.[28] inflammatory cytokines (TNF-α and IL-6) were quantified by the enzyme-linked immunosorbent assay method using commercial kits (Krishgen Biosystems).

Histological analysis

The colon tissue at the distal end was fixed for 24 hours in a 10% *v/v* formaldehyde solution and later embedded in paraffin. The sections were cut, and hematoxylin and eosin were used to stain them. The slides were examined under a light microscope.

Statistical analysis

All the data were expressed as the mean ± standard deviation. Data analysis was carried out using the GraphPad Prism 9.0 software package (GraphPad, San Diego, CA). The parametric variables were analysed using one-way ANOVA, followed by Dunnett's post hoc analysis. Student's t-test was used to compare two groups. A value of $p<0.05$ was considered to be statistically significant.

RESULTS

Marmelosin content in AME

HPTLC analysis was conducted to quantify AME by determining the marker compound, marmelosin (Figure 1). The marmelosin content in AME was determined using the standard calibration graph (Figure 2). It was found to be 0.349±0.03% *w/w*.

Phytosome formulation

Fifteen formulations were prepared using a second-order Box-Behnken design at three levels, and their entrapment efficiencies were determined. The independent variables and their levels in the formulation are provided in Table 1. The layout of the experiment design is shown in Table 2. The entrapment efficiencies of 15 formulations varied between 23.02% *w/w* and 82.77% *w/w*.

A linear model was chosen for analyzing the variable response as it had a comparatively higher R^2 value (0.9523) and a lower predicted residual sum of squares (PRESS) value.[29] The mathematical relationship as given by Design-Expert 13.0.5.0 for the measured responses is: Entrapment efficiency = +57.82-1.43*A+15.87*B+12.05*C (2).

Where A is the AME:PC ratio, B is the temperature, and C is the stirring time. The sign and value of the coefficients in equation (2) represent the tendency and magnitude of the factors' influence on the response. If the value is positive, there is a direct correlation between the factor and the response; if it is negative, there is an inverse correlation. The contour plots showing the relationship between entrapment efficiency and the independent variables can be observed in Figure 3.

The model's *f* value of 73.27 and *p* value of less than 0.0001 imply that the model is significant (Table 3). The lack-of-fit *f* value of 8.30 indicates that it is not significant in comparison to the pure error. For a good model, a non-significant lack of fit is generally considered desirable. The predicted R^2 value of 0.9125 is in reasonable agreement with the adjusted R^2 value of 0.9393, *i.e.*, the difference is less than 0.2. Adeq Precision measures the signal-to-noise ratio, which should preferably be above 4.[30] The ratio of 28.7318 indicates an adequate signal, and the model can be used to navigate the design space. The optimised formulation of AMEP was developed by

Design Expert software based on desirability criteria. The predicted value of the optimised formulation as generated by the software was 82.77% *w/w*, which similar to the actual value of formulation F6. Hence, formulation F6 was selected as the optimized batch. The optimal values of the independent variables, *i.e.*, AME-to-phospholipid ratio *(w/w)*, reaction temperature (°C), and reaction time (hours), were found to be 1:1, 55 °C, and 3 h, respectively.

Validation of the optimised model

An additional batch of AMEP was prepared using optimised independent variables to validate the model. Its entrapment efficiency was determined. The predicted entrapment efficiency obtained from the developed model and the actual values of entrapment efficiency achieved from the prepared formulation were compared. The model-predicted value of EE (%) of marmelosin in the optimized formulation of AMEP was found to be 85.16%, while the actual EE (%) from the prepared formulation of AMEP was found to be 83.15±1.04%. Thus, the

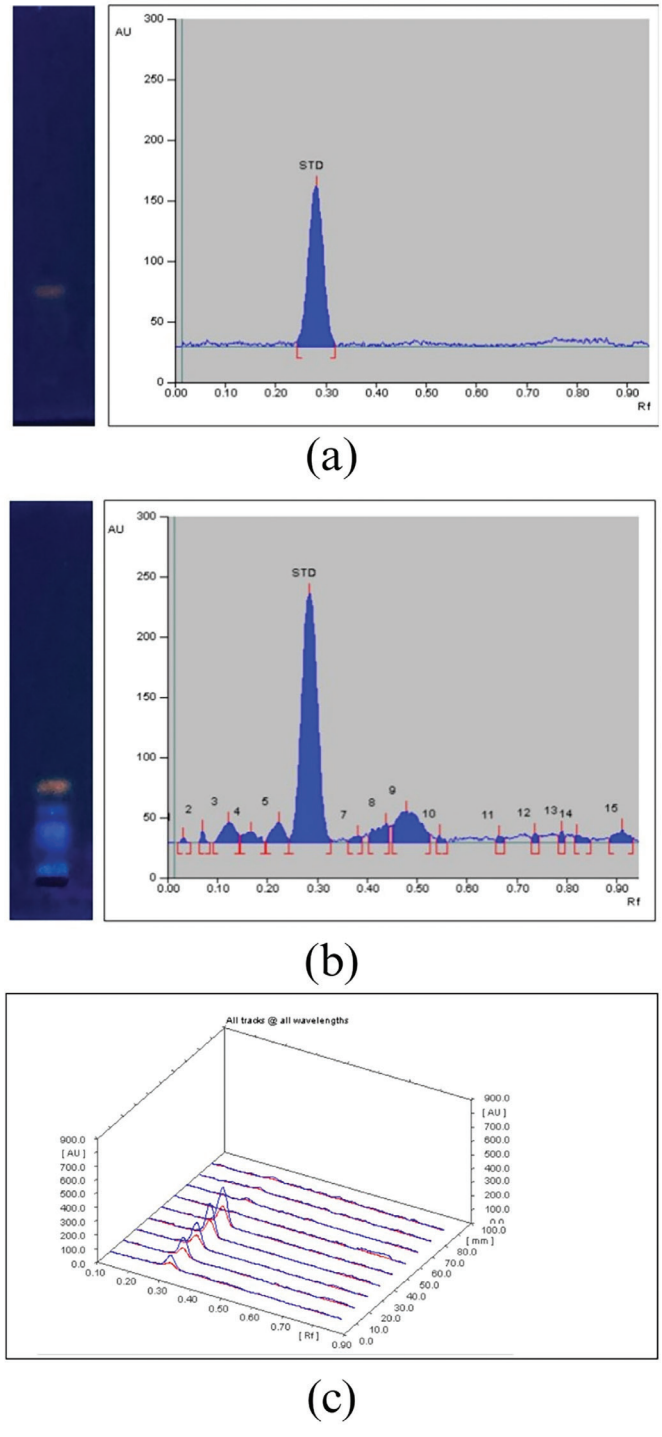

Figure 1. HPTLC chromatograms for marmelosin determination of determination of marmelosin in extract (AME). HPTLC chromatograms of (a) standard marker (marmelosin) at 366 nm; (b) AME at 366 nm; (c) 3D overlay of HPTLC chromatogram of all tracks at 254 nm (red graphs) and 366 nm (blue graphs)

HPTLC: High-performance thin layer chromatography, AME: *Aegle marmelos* fruit extract

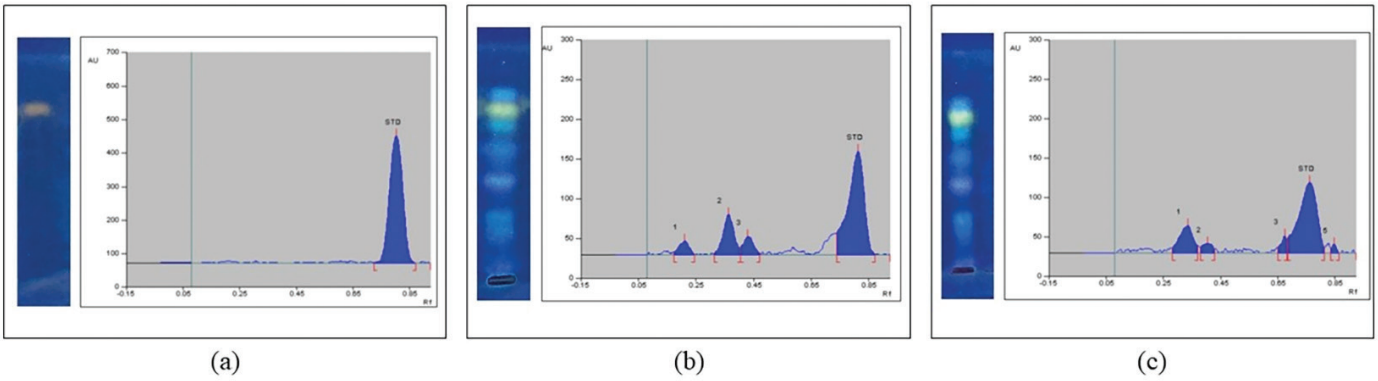

Figure 2. HPTLC chromatogram for entrapment efficiency of marmelosin formulation at 366 nm of determination of entrapment efficiency of marmelosin in formulations at 366 nm. HPTLC chromatographs of (a) standard marker (marmelosin); (b) AME; (c) AMEP

HPTLC: High-performance thin layer chromatography, AMEP: *Aegle marmelos* fruit extract-phospholipid

Table 1. Coded levels and real values for each factor

Independent variable	Actual levels at coded factor levels		
	-1	0	+1
Extract: Phospholipid ratio	1:1	2:1	3:1
Temperature (°C)	35	45	55
Stirring time (h)	1	2	3

applicability of the developed model was validated. The bias (%) was calculated using equation 3 and was found to be less than 3%,[31] suggesting the relative robustness of the model.

$$\text{Bias (\%)} = \frac{\text{predicted value} - \text{observed value}}{\text{predicted value}} \times 100 \quad (3)$$

The predicted and observed entrapment efficiency of AMEP prepared using optimised parameters is given in Table 4. The result confirms the precision and validity of the response surface methodology for the AMEP formulation method.

Solubility profile

The solubility profiles of PC, AME, and AMEP show that PC is soluble in organic solvents, while AME is soluble in polar solvents. Details regarding AMEP's solubility are not provided. AMEP forms micelles in aqueous solutions and is soluble in chloroform.

SEM, particle size, FTIR, and DSC analysis

SEM analysis was performed to observe the surface morphology. The AMEP was dispersed in water before observation under SEM. The electron micrographs showed spherical, uniform vesicles of AMEP (Figure 4a). These spherical vesicles were observed as discrete structures without aggregation.

The particle size of the dispersed AMEP was found to be 673.6±4.30 nm, and its PI was 0.224±0.010 (Figure 4b). The zeta potential was found to be -42.6 mV±0.51 (Figure 4c).

The FTIR and DSC graphs of AME, PC, PM, and AMEP are shown in Figure 5a, b.

In vivo study

DAI, weight loss and colon length

The DAI scores of all groups except the normal group increased in the first 7 days (Figure 6a). The DAI score of the positive-control or DSS group increased consistently and remained higher even on Day 14. The DAI scores of the standard-treated and AMEP-treated groups decreased more, compared with the AME-treated and excipient-treated groups, indicating better amelioration of symptoms of colitis. The animals showed progressive weight loss in the first 7 days as they consumed DSS. Weight loss in colitis is due to the loss of body fluids (diarrhea and colorectal bleeding), malabsorption, and decreased appetite, which leads to nutrient deficiencies.

The DSS group had the maximum weight loss (about 15.0%), while the standard group had the minimum weight loss (5.12%) (Figure 6b). When compared with the standard group, the weight loss was significantly lower in the AMEP-treated group (p=0.0026) compared to the AME-treated group (p<0.0001) and the excipient-treated group (p<0.0001).

The length of the colon in all the DSS-consuming groups was shorter than in the normal group. The colon length of the DSS group was found to be significantly shorter relative to the normal group (p<0.0001). The colon lengths of the standard-treated group (G-III) and the AMEP-treated group (G-V) were not significantly different (p=0.3107), however, the colon lengths of the standard group and the AME group are significantly different (p<0.05) (Figure 6c).

Biochemical evaluation

Animals consuming DSS showed increased levels of NO in colon tissues. The NO level of the DSS group was significantly higher. The NO level in all the treated groups decreased significantly compared to the DSS group. The NO level was lowest in the standard-treated group. No significant difference was observed between the decreased NO level of the standard group and the AMEP-treated group (p=0.1161). However, the difference between the NO level of the standard group and the AME-treated group was significant (p<0.0001) (Figure 7a). The SOD level of the colonic tissues decreased significantly in the DSS group (p<0.001, compared with the normal group). These changes

Table 2. Composition of experimental formulations obtained using Box-Behnken design for AMEP and their respective entrapment efficiency

Formulation	Extract: Phospholipid ratio	Temperature (°C)	Stirring time (h)	Observed entrapment efficiency* (*w/w* %)	Predicted entrapment efficiency (*w/w* %)
F1	-1	0	-1	49.75±0.95	47.20
F2	0	0	0	62.75±0.32	57.82
F3	-1	1	0	71.68±0.44	75.12
F4	1	-1	0	42.31±0.83	40.52
F5	1	0	1	67.62±0.87	68.44
F6	-1	1	1	82.77±1.05	87.16
F7	1	1	0	71.57±0.43	72.27
F8	0	-1	1	51.44±0.65	53.99
F9	0	0	0	60.17±0.41	57.82
F10	0	1	-1	63.15±0.98	61.65
F11	-1	-1	0	43.98±0.67	43.37
F12	1	0	-1	41.99±0.62	44.35
F13	0	-1	-1	23.02±0.89	29.90
F14	0	0	0	62.65±0.30	57.82
F15	-1	0	1	73.87±0.94	71.29

*Each value represents the mean ± standard deviation (n=3), AMEP: *Aegle marmelos* fruit extract-phospholipid

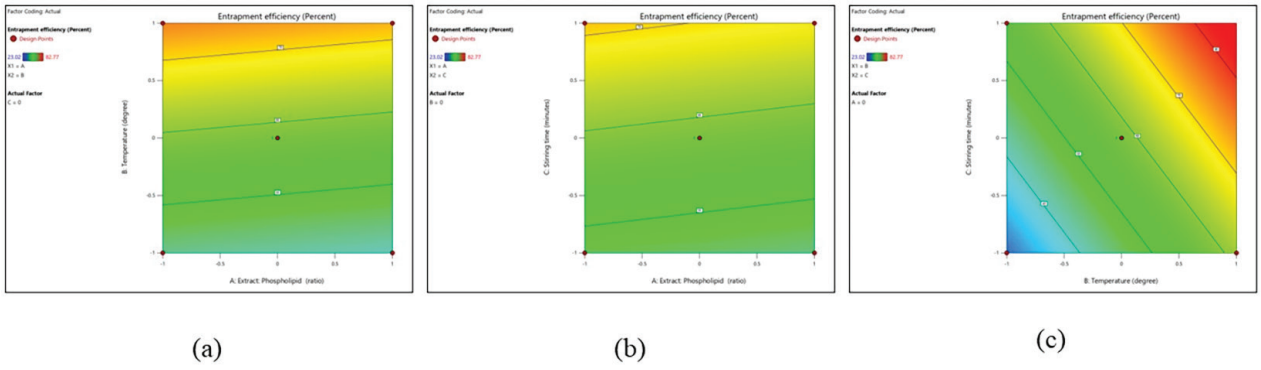

Figure 3. Contour plots showing effect of independent variables on entrapment efficiency (a) temperature and extract to phospholipid ratio; (b) stirring time and extract to phospholipid ratio; (c) stirring time and temperature

were significantly mitigated by the AME-treated, AMEP-treated, and standard groups (with $p<0.05$, 0.01, and 0.01, respectively), as compared with the normal control group (Figure 7b). DSS consumption significantly increased the colonic MDA level in all the groups ($p<0.0001$, compared with the normal group). This change was reversed in all the treated groups and was most decreased by the standard-treated group. The decreased MDA level in the standard group was not significant ($p=0.4396$), compared with the decreased MDA level in the AMEP group, but it was significant ($p<0.05$) compared with that of the AME group. Thus, AMEP decreased the MDA level more efficiently than AME. This could be because of the better bioavailability of the extract complex compared with the plain extract (Figure 7c).

The levels of the pro-inflammatory cytokines TNF-α and IL-6 increased with DSS intake. These levels increased significantly in the DSS group compared with the normal group ($p<0.001$). These increases were reduced by standard, AME, and AMEP treatments. The TNF-α reduction compared with the DSS group was highly significant in the AMEP-treated and standard-treated groups ($p<0.0001$ in both), significant in the AME-treated group ($p<0.01$), and not significant in the excipient-treated group ($p=0.2238$) (Figure 7d). The IL-6 reduction was highly significant in the standard-treated group and the AMEP-treated group ($p<0.0001$, both) compared with the DSS-treated group, but it was not significantly reduced in the AME-treated group or the excipient-treated group ($p=0.2886$, 0.6306, respectively) (Figure 7e).

Table 3. ANOVA and fit statistics results

Source	Sum of squares	Mean square	*f* value	*p* value
Model	3274.44	1091.48	73.27	<0.0001*
A. Extract: Phospholipid ratio	17.62	17.62	1.18	0.3000
B. Temperature	1987.37	1987.37	133.41	<0.0001
C. Stirring time	1144.32	1144.32	76.82	<0.0001
Residual	163.86	14.90		
Lack of fit	159.59	17.73	8.30	0.1121#
Fit statistics				
SD	3.86			
R^2	0.9523			
Adjusted R^2	0.9393			
Predicted R^2	0.9125			
Adeq precision	28.7318			

*: Significant, #: Not significant, ANOVA: Analysis of variance, SD: Standard deviation

Table 4. Predicted and observed entrapment efficiency of AMEP prepared using optimised parameters

Response variable	Predicted values (*w/w* %)	Observed values* (*w/w* %)	
Entrapment efficiency	85.16	83.15 ± 1.04	2.36

*: Mean ± standard deviation (n=3), AMEP: *Aegle marmelos* fruit extract-phospholipid

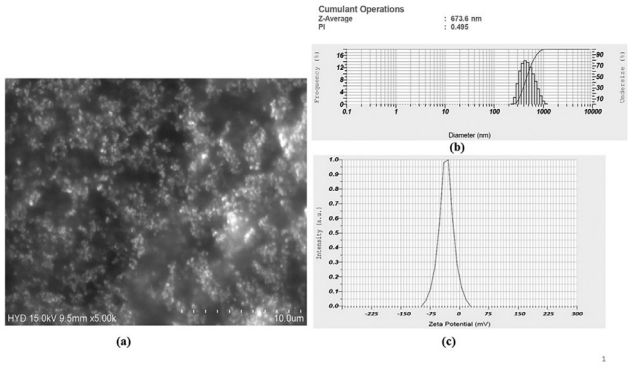

Figure 4. Characterization of optimised AMEP: (a) SEM; (b) particle size and particle index; and (c) zeta potential

AMEP: *Aegle marmelos* fruit extract-phospholipid, SEM: Scanning electron microscopy

Histopathology

The colon architecture was disrupted noticeably in the DSS-treated group (Figure 8). This disruption could be characterized as edema, crypt damage, cell infiltration, ulceration, and sub-mucosal erosion. The standard and AMEP-treated groups had fewer infiltrating cells and suffered less mucosal damage compared with the DSS-treated group. Thus, animals that were treated with the standard treatment and AMEP experienced considerable protection of colon tissue compared with the other groups.

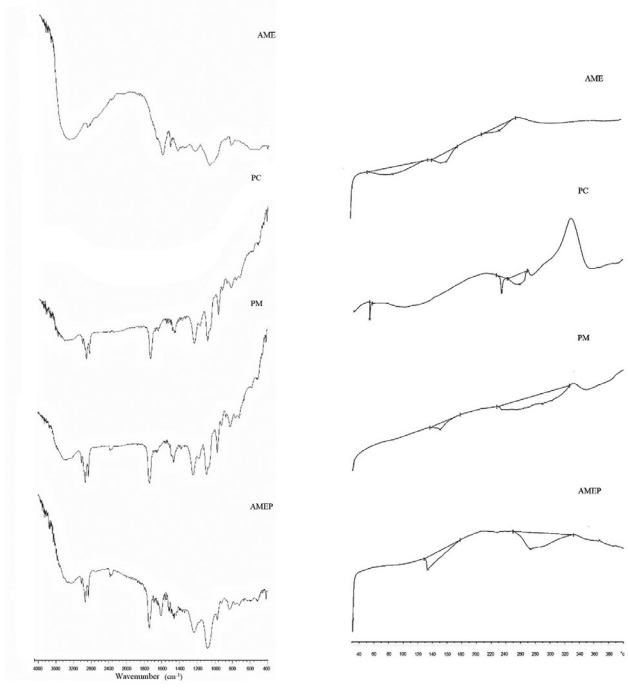

Figure 5. (a) FTIR graphs and (b) thermograms of AME, PC, a PM, and the optimised AMEP formulation

FTIR: Fourier transform infrared spectroscopy, PM: Physical mixture, AMEP: *Aegle marmelos* fruit extract-phospholipid, PC: Phosphatidylcholine

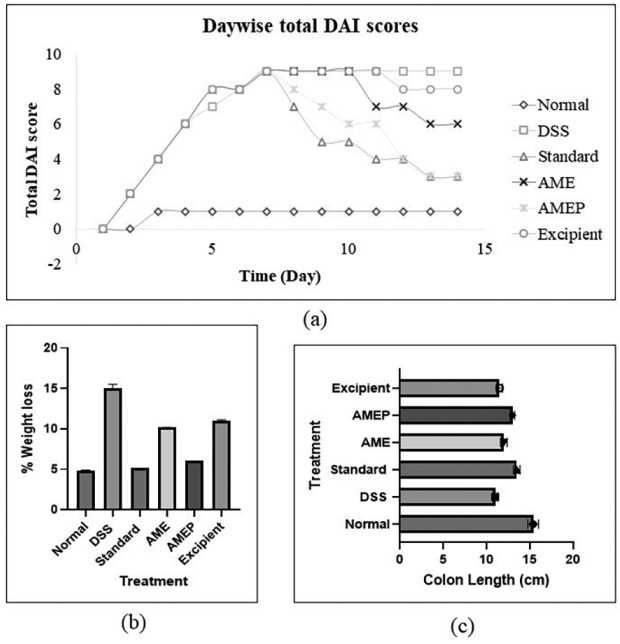

Figure 6. (a) Total DAI scores; (b) weight loss; and (c) colon length in colitis-induced rats
DAI: Disease Activity Index

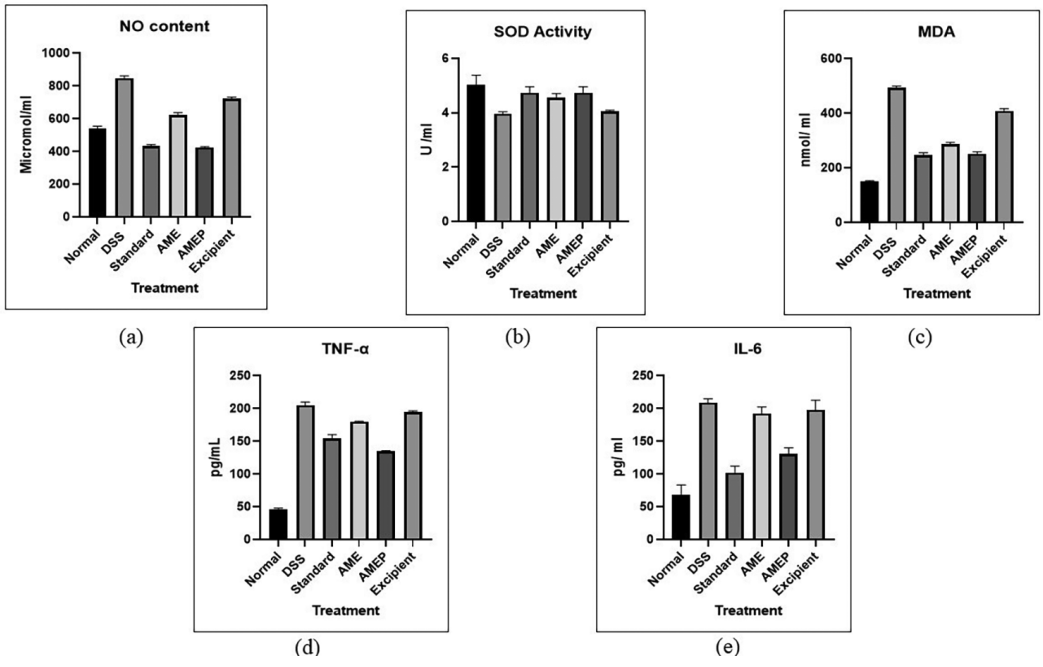

Figure 7. Concentrations of (a) NO; (b) SOD; (c) MDA; (d) TNF-α; and (e) IL-6 levels in rat colon tissues
NO: Nitric oxide, MDA: Malondialdehyde, SOD: Superoxide dismutase, TNF-α: Tumor necrosis factor-alpha, IL-6: Interleukin

DISCUSSION

The parameters that played a significant role in AMEP formulation were the AME to phospholipid ratio *(w/w)*, reaction temperature (°C), and reaction time (hours). The molar ratio of AME-to-phospholipid was not used in the study because of the diverse phytoactives present in AME. The scatterplots of these parameters revealed that there was no correlation between them.

Observing equation (2), it is clear that variables B (temperature) and C (reaction time) have a positive effect, while variables A (AME:PC ratio) have a negative effect on the entrapment efficiency of AMEP. A higher AME:PC ratio decreases entrapment efficiency. An increase in PC increased the complexation. However, higher PC concentrations made the product viscous, so ratios of AME:PC less than 1:1 were not studied. As the concentration of AME increased, the entrapment efficiency did not increase. The AME powder precipitated on the surface of

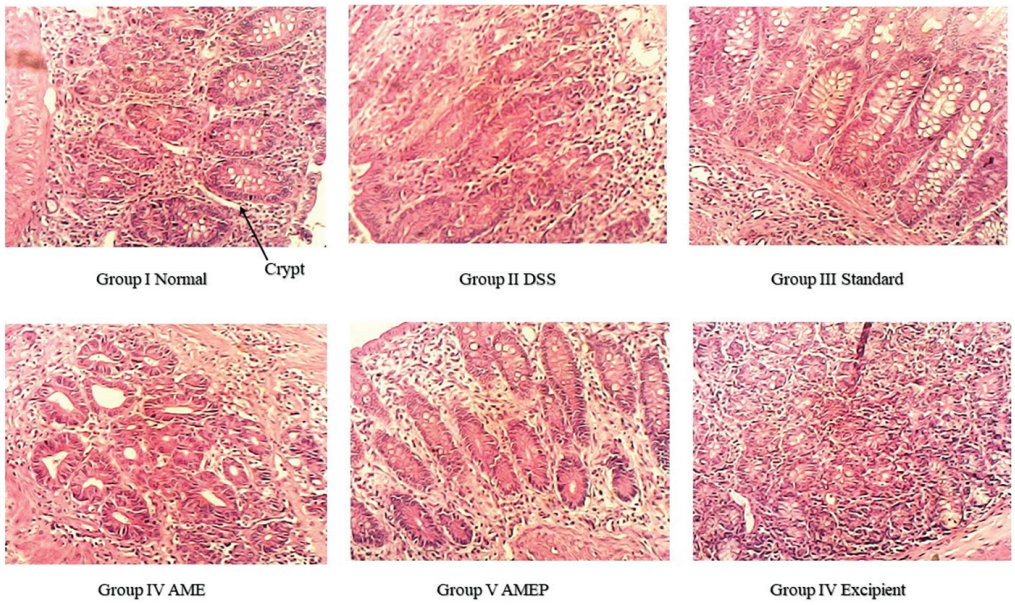

Figure 8. Histopathology of colitis-induced rats
DSS Dextran sulfate sodium, AMEP: A. marmelos fruit extract-phospholipid

the RBF as the ratio of AME to PC increased. This may be due to incomplete entrapment of AME and an insufficient amount of PC to associate with AME. Thus, the weight-by-weight ratio of 1:1 between AME and PC gave maximum entrapment efficiency. The entrapment efficiency of AMEP increased with an increase in temperature. This may be due to the increased melting of lipid at higher temperatures, which led to a decrease in its viscosity. The movement of lipid increased due to its reduced viscosity, leading to interaction with AME, forming an association. Increased stirring time improved the entrapment efficiency, which may be because of increased reaction time and enhanced movement of molecules, leading to augmented complex formation of AME and PC molecules.

The zeta potential is the surface charge of the particles. It helps assess the stability of a formulation. Values greater than -30 mV indicate good physical stability and are considered acceptable.[32] The stability of the dispersed AMEP was found to be acceptable.

In Figure 5a, the region of the FTIR spectra between 3400 and 3200 cm^{-1} shows characteristic peaks of polyphenolic compounds that are due to the polymeric hydroxyl group and hydrogen bond stretching.[33] This can be observed in the AME spectrum as intense peaks in the 3384-3203 cm^{-1} range. The -CH, -CH2, and -CH3 stretching can be observed in the 2950–2850 cm^{-1} range. The FTIR peaks at 1604 and 1560 cm^{-1} are due to aromatic bond stretching, whereas the peaks near 1200 cm^{-1} are due to phenolic C-O stretching. The FTIR spectrum of PC exhibits characteristic peaks of alkanes in the 2931-2854 cm^{-1} region, C=O stretching at 1734 cm^{-1}, P=O stretching at 1244 cm^{-1}, P-O-C stretching at 1089 cm^{-1}; and -N+(CH3)3 stretching at 968 cm^{-1}. The AME and PC peaks in the PM show additive effects, in which almost all the peaks of AME and PC have combined without shifting any peak. However, the FTIR graph of AMEP shows a shift of the P=O peak from 1244 to 1232 cm^{-1} and a shift of the P-O-C peak from 1089 to 1081 cm^{-1}. This may be due to hydrogen bond formation between hydrophilic polyphenols, present in AME, and the polar phosphate head of PC. Also, in the FTIR spectrum of AMEP, the intensity of the peak at 1604 cm^{-1} has changed, and the peak at 1560 cm^{-1} has disappeared, which indicates aromatic ring stretching. This may be influenced by polar covalency, leading to the weakening, withdrawing, or shielding of electrons in bonds. This behaviour may be caused by the packing of AME molecules in the hydrophobic cavity of PC. The AME molecules may be held by Van der Waals forces and hydrophobic interactions. Thus, the FTIR spectrum of AMEP suggests two possible interactions between AME molecules and PC. The first hydrophilic interaction is between the polar head of PC and polyphenols in AME; the second hydrophobic interaction is between the non-polar tail of PC and aromatic molecules in AME.[34]

DSC was used to examine interactions among the components used in the formulation (Figure 5b). The endothermic peaks of AME, PC, PM, and AMEP were observed. The disappearance of existing peak(s), the appearance of new peak(s), altered peak shape, altered onset of a peak, altered peak temperature, and relative peak area or enthalpy signifies an interaction in a DSC.[35] The thermogram of PC shows two sharp endothermic peaks at 55.28 °C and 234.94 °C. The first peak is mostly the melting point of PC, and the second peak is due to phase transitions, *i.e.*, isomeric or crystalline changes in the PC molecule. The AME thermogram shows broad endothermic peaks at 89.12 °C, 161.46 °C, and 234.01 °C. However, the AMEP thermogram shows two peaks at 133 °C and 273.46 °C, which are different from those observed in PC and AME. The interaction of AME with PC may have led to the disappearance of the second endothermic peak

of PC. The DSC of AMEP shows significant reductions in the enthalpy and the melting points of AME and PC. It has been reported that hydrogen bonds can be established between the hydroxyl groups of polyphenols and the polar head of PC.[36] Thus, hydroxyl groups of phenolic moieties in AME could be involved in hydrogen bonding, while aromatic rings could be involved in hydrophobic bonding. The interaction of polyphenol hydroxyl groups of AME with the polar head of PC may allow the hydrocarbon tail of PC to wrap around the polar head of PC, which contains polyphenol molecules. This may lead to the disappearance of the individual peaks of PC and AME, as well as the appearance of two distinct sharp peaks, which may be due to AMEP formation.

The DSS rat model was used to induce colitis. DSS is a sulfated polysaccharide with colitogenic activity. Intestinal inflammation results from damage to the colonic epithelial layer, allowing intestinal contents to infiltrate the underlying tissue and trigger inflammation.

The animals were observed for symptoms of colitis. The animals in the different groups consuming DSS developed symptoms of colitis to various degrees. The symptoms of colitis that were induced included increased DAI, reduced body weight, and reduced colon length. Administration of DSS also caused histological damage through surface epithelial damage, loss of goblet cells, and infiltration of inflammatory cells. The antioxidant activities of the colon tissues were decreased. This could be observed as elevated levels of MDA and NO, a decreased SOD level, and increased levels of proinflammatory cytokines (TNF-α, IL-6).[37] SOD has an antioxidant function, and a decrease in the SOD level corresponds to oxidative damage. MDA is an indicator of oxidative damage, and the MDA level is proportional to the damage.[38] The levels of oxidative stress markers (NO, SOD, and MDA) in the AMEP-treated groups were comparable to those of the standard-treated group. These levels were better controlled by AMEP than by AME. AMEP managed the anti-inflammatory cytokines more efficiently than AME.

The phytoactives exhibit poor oral bioavailability due to their poor solubility. PC being amphiphilic increases the drug solubility by its wetting function and decreases the interfacial tension between the phytoactives and the aqueous environment. The phospholipid complex formation also reduces the crystallinity of the phytoactives, and the increased amorphous nature of the complex may lead to improved solubility of the phytoactives. The phospholipid complexes have high dispersibility, which could be another reason for the improved hydrophilicity of phytoactives. Thus, improved oral bioavailability of the phytoactives may have been attributed to;

• The potential of PC to act as a chaperone molecule to cross the biological membranes and hence improve the absorption and bioavailability of phytoactives.

• The dissolution rate of poorly soluble phytoactives was improved. For poorly soluble drugs, solubility is the rate-limiting step in drug absorption.

• The increased lipophilicity and hydrophilicity of phytoactives which may have enhanced the penetration of phytoactives into intestinal mucosa and/or increased the rate and amount of phytoactives in gastrointestinal fluids, respectively.

The *in vivo* investigations have demonstrated that the anti-colitis activity of AMEP is superior to that of AME. The greater potency can be attributed to the enhanced lipophilic nature of phospholipid complexes, leading to improved bioavailability of the phytoactives.

CONCLUSION

The fruit of *A. marmelos* is underutilised with potential medicinal use. Although it is used in ethnomedicine to alleviate gastrointestinal disorders, its commercial utility for treating colitis has never been explored.

In the current study, *A. marmelos* fruit extract was prepared using a simple maceration technique, and its activity was enhanced by complexing it with phospholipid, using an easy, reproducible, and economical method.

Potential antioxidants and anti-inflammatory phytoconstituents were found in the extract. The extract was quantified, and phospholipid complexes of the extract were formulated and optimized. The *in vivo* activities of the phospholipid complexes of the extract were found to be significantly higher than the plain extract. These findings were supported by the histopathological examination of the colon. Thus, the formulation significantly improves the antioxidant and anti-inflammatory activities of AME. The activity was comparable with that of conventional mesalamine.

It can be concluded that the phospholipid complexes, of *A. marmelos* fruit extract, may provide convenient and safer alternatives to the conventional drugs used in the treatment of UC. The research may stimulate the development of commercial formulations containing phospholipid complexes of phytoactives for the treatment of UC.

Ethics

Ethics Committee Approval: Practical procedures were performed in compliance with the CPCSEA, Government of India, and, as approved by the Institutional Animal Ethic Commitee study protocol (approval number: 535/PO/RERCBT/S/02/CPCSEA/IPER/IAEC/2020-2021/17, date: 19.12.2020).

Informed Consent: Not required.

Acknowledgment

For supporting the project under the Women Scientist Scheme A (WOS-A) programme (DST/WOS-A/LS-73/2020), the authors are grateful to the Department of Science and Technology (DST), Government of India. The authors are thankful to Lipoid GmbH, Ludwigshafen, for providing gift samples of phosphatidylcholine (Lipoid H90).

Footnotes

Authorship Contributions

Concept: P.G.S., Design: P.G.S., D.J.S., Data Collection or Processing: P.G.S., Analysis or Interpretation: P.G.S., D.J.S., R.O.G., Literature Search: P.G.S., Writing: P.G.S., D.J.S, R.O.G.

Conflict of Interest: The authors declare no conflicts of interest.

Financial Disclosure: The authors declared that this study received no financial support.

REFERENCES

1. Ungaro R, Mehandru S, Allen PB, Peyrin-Biroulet L, Colombel JF. Ulcerative colitis. Lancet. 2017;389:1756-1770.
2. Langan RC, Gotsch PB, Krafczyk MA, Skillinge DD. Ulcerative colitis: diagnosis and treatment. Am Fam Physician. 2007;76:1323-1330.
3. Torres J, Billioud V, Sachar DB, Peyrin-Biroulet L, Colombel JF. Ulcerative colitis as a progressive disease: the forgotten evidence. Inflamm Bowel Dis. 2012;18:1356-1363.
4. Bilsborough J, Targan SR, Snapper SB. Therapeutic targets in inflammatory bowel disease: current and future. Am J Gastroenterol Suppl. 2016;3:27-37.
5. Ferretti F, Cannatelli R, Monico MC, Maconi G, Ardizzone S. An update on current pharmacotherapeutic options for the treatment of ulcerative colitis. J Clin Med. 2022;11:2302.
6. Al-Bawardy B, Shivashankar R, Proctor DD. Novel and emerging therapies for inflammatory bowel disease. Front Pharmacol. 2021;12:651415.
7. Lin SC, Cheifetz AS. The use of complementary and alternative medicine in patients with inflammatory bowel disease. Gastroenterol Hepatol. 2018;14:415-425.
8. Navaneethan U, Shen B. Pros and cons of medical management of ulcerative colitis. Clin Colon Rectal Surg. 2010;23:227-238.
9. Atanasov AG, Waltenberger B, Pferschy-Wenzig EM, Linder T, Wawrosch C, Uhrin P, Temml V, Wang L, Schwaiger S, Heiss EH, Rollinger JM, Schuster D, Breuss JM, Bochkov V, Mihovilovic MD, Kopp B, Bauer R, Dirsch VM, Stuppner H. Discovery and resupply of pharmacologically active plant-derived natural products: a review. Biotechnol Adv. 2015;33:1582-1614.
10. Murthy HN, Bhat MA, Dalawai D. Bioactive compounds of bael [*Aegle marmelos* (L.) Correa]. In: Murthy HN, Bapat V, eds. Bioactive compounds in underutilized fruits and nuts. Springer, Cham. Reference Series in Phytochemistry. 2019:1-28.
11. Baliga MS, Thilakchand KR, Rai MP, Rao S, Venkatesh P. *Aegle marmelos* (L.) Correa (Bael) and its phytochemicals in the treatment and prevention of cancer. Integr Cancer Ther. 2013;12:187-196.
12. Bulani VD, Kothavade PS, Kundaikar HS, Gawali NB, Chowdhury AA, Degani MS, Juvekar AR. Inclusion complex of ellagic acid with β-cyclodextrin: characterization and *in vitro* anti-inflammatory evaluation. J Mol Struct. 2016;1105:308-315.
13. Bruni R, Barreca D, Protti M, Brighenti V, Righetti L, Anceschi L, Mercolini L, Benvenuti S, Gattuso G, Pellati F. Botanical sources, chemistry, analysis, and biological activity of furanocoumarins of pharmaceutical interest. Molecules. 2019;24:2163.
14. Pynam H, Dharmesh SM. Antioxidant and anti-inflammatory properties of marmelosin from bael (*Aegle marmelos* L.): inhibition of TNF-α mediated inflammatory/tumor markers. Biomed Pharmacother. 2018;106:98-108.
15. Jiang Y, Fang H, Lin S, Chen Y, Fu Y, Tu Y, Li Q, Hui Z. Imperatorin inhibits LPS-induced bone marrow-derived macrophages activation by decreased NF-κB p65 phosphorylation. Immunopharmacol Immunotoxicol. 2023;45:581-588.
16. Ma T, Liu P, Wei J, Wei J, Zhao M, Yao X, Luo X, Xu S. Imperatorin alleviated endometriosis by inhibiting the activation of PI3K/Akt/NF-κB pathway in rats. Life Sci. 2021;274:119291.
17. Luo M, Luo Y. Imperatorin relieved ulcerative colitis by regulating the Nrf-2/ARE/HO-1 pathway in rats. Inflammation. 2021;44:558-569.
18. Liang X, Chen X, Zhao G, Tang T, Dong W, Wang C, Zhang J, Liao Z. Preparation, characterization, and pharmacokinetic evaluation of imperatorin lipid microspheres and their effect on the proliferation of MDA-MB-231 cells. Pharmaceutics. 2018;10:236.
19. Byeon JC, Ahn JB, Jang WS, Lee SE, Choi JS, Park JS. Recent formulation approaches to oral delivery of herbal medicines. J Pharm Investig. 2019;49:17-26.
20. Kuche K, Bhargavi N, Dora CP, Jain S. Drug-phospholipid complex: a go-through strategy for enhanced oral bioavailability. AAPS PharmSciTech. 2019;20:1-13.
21. Song JG, Noh HM, Lee SH, Han HK. Lipid/clay-based solid dispersion formulation for improving the oral bioavailability of curcumin. Pharmaceutics. 2022;14:2269.
22. Tan Q, Liu S, Chen X, Wu M, Wang H, Yin H, He D, Xiong H, Zhang J. Design and evaluation of a novel evodiamine-phospholipid complex for improved oral bioavailability. AAPS PharmSciTech. 2012;13:534-547.
23. Gnananath K, Nataraj KS, Rao GB. Phospholipid complex technique for superior bioavailability of phytoconstituents. Adv Pharm Bull. 2017;7:35-42.
24. Jia X, Gao Y, Liu L, Guo Y, Wang J, Ma H, Zhao R, Li B, Du Y, Yang Q. Artemisinin alleviates intestinal inflammation and metabolic disturbance in ulcerative colitis rats induced by DSS. Evid Based Complement Alternat Med. 2022;2022(1):6211215.
25. Nishiyama Y, Kataoka T, Yamato K, Taguchi T, Yamaoka K. Suppression of dextran sulfate sodium-induced colitis in mice by radon inhalation. Mediators Inflamm. 2012;2012:239617.
26. Montgomery HAC, Dymock JF. The rapid determination of nitrate in fresh and saline waters. Analyst. 1962;87:374-378.
27. Mesa-Herrera F, Quinto-Alemany D, Díaz M. A sensitive, accurate, and versatile method for the quantification of superoxide dismutase activities in biological preparations. React Oxyg Species. 2019;7:10-20.
28. Kowalczuk K, Stryjecka-Zimmer M. The influence of oxidative stress on the level of malondialdehyde (MDA) in different areas of the rabbit brain. Ann Univ Mariae Curie-Sklodowska Med. 2002;57:160-164.
29. Swamy GJ, Sangamithra A, Chandrasekar V. Response surface modeling and process optimization of aqueous extraction of natural pigments from *Beta vulgaris* using Box-Behnken design of experiments. Dyes Pigm. 2014;111:64-74.
30. Miranda G, Faria S, Bartolomeu F, Pinto E, Madeira S, Mateus A, Carreira P, Alves N, Silva FS, Carvalho O. Predictive models for physical and mechanical properties of 316L stainless steel produced by selective laser melting. Mater Sci Eng A. 2016;657:43-56.
31. Qin X, Yang Y, Fan TT, Gong T, Zhang XN, Huang Y. Preparation, characterization and *in vivo* evaluation of bergenin-phospholipid complex. Acta Pharmacol Sin. 2010;31:127-136.
32. Shah R, Eldridge D, Palombo E, Harding I. Optimisation and stability assessment of solid lipid nanoparticles using particle size and zeta potential. J Phys Sci. 2014;25:59-75.
33. Wongsa P, Phatikulrungsun P, Prathumthong S. FT-IR characteristics, phenolic profiles and inhibitory potential against digestive enzymes of 25 herbal infusions. Sci Rep. 2022;12:6631.
34. Mignet N, Seguin J, Chabot GG. Bioavailability of polyphenol liposomes: a challenge ahead. Pharmaceutics. 2013;5:457-471.

35. Maiti K, Mukherjee K, Gantait A, Saha BP, Mukherjee PK. Curcumin-phospholipid complex: preparation, therapeutic evaluation and pharmacokinetic study in rats. Int J Pharm. 2007;330:155-163.

36. Karonen M. Insights into polyphenol-lipid interactions: chemical methods, molecular aspects and their effects on membrane structures. Plants. 2002;11:1809.

37. Pavan E, Damazo AS, Arunachalam K, Almeida PO de A, Oliveira DM, Venturini CL, Figueiredo F de F, Cruz TCD da, Silva JV da, Martins DT de O. *Copaifera malmei* Harms leaves infusion attenuates TNBS-ulcerative colitis through modulation of cytokines, oxidative stress and mucus in experimental rats. J Ethnopharmacol. 2021;267:113499.

38. Tsikas D. Assessment of lipid peroxidation by measuring malondialdehyde (MDA) and relatives in biological samples: analytical and biological challenges. Anal Biochem. 2017;524:13-30.